Electronic Supplementary Material (ESI) for Dalton Transactions.

Monitoring Structure and Coordination Chemistry of Co_4O_4-based Oxygen Evolution Catalysts by Nitrogen-14/-15 and Cobalt-59 NMR Spectroscopy

1. Methods and materials

Benzonitrile (for synthesis), cobalt nitrate hexahydrate (98%), hydrogen peroxide (35%), potassium hexacyanocobaltate(III) (98%), pyridine (98%), {^{15}N}pyridine (98 atom % 15N), sodium acetate trihydrate (for analysis) and sodium persulfate (reagent grade, ≥98%) were purchased from Sigma-Aldrich, sodium tetraborate decahydrate (≥98%) from Carl Roth and tris(2,2'-bipyridyl)ruthenium(II) Chloride Hexahydrate (>98%) and 2,4,6-tri(4-pyridyl)-1,3,5-triazine (purified by sublimation, ≥97%) from TCI. All chemicals were used as received. Deuterated solvents were purchased from Deutero or Eurisotop.

Liquid NMR spectra were recorded either on a Bruker Ascend 400 spectrometer (9.4 T, ^{1}H at 400.13 MHz, ^{13}C at 100.61 MHz, ^{15}N at 40.54 MHz, ^{59}Co at 94.94 MHz), a Bruker Avance III 600 HD spectrometer (14.1 T, ^{1}H at 600.25 MHz, ^{15}N at 60.82 MHz) or on a JEOL ECX400 spectrometer (9.4 T, ^{1}H at 399.60 MHz, ^{13}C at 100.47 MHz, ^{15}N at 40.49 MHz, ^{59}Co at 93.78 MHz). Proton-1 and carbon-13 spectra were referenced against the residual solvent signal, cobalt-59 spectra were referenced against saturated $K_3[Co(CN)_6]$ in D_2O, and nitrogen-15 chemical shifts were referenced using the unified scale as recommended by IUPAC.[1,2]

IR spectra were recorded using a Thermo Scientific™ Nicolet™ iS™5 FT-IR spectrometer, as KBr pellets in transmission with a resolution of 1 cm^{-1} and 16 scans per sample.

CHN analysis were performed on a Vario micro cube (Elementar Analysensysteme GmbH).

2. $Co_4O_4(OAc)_4Py_4$ synthesis

The synthesis was done according to a modified literature procedure:[3]

In a 100 ml 3-neck round-bottom flask equipped with a reflux condenser 2.96 g (10.0 mmol) $Co(NO_3)_2 \cdot 6\ H_2O$ and 2.81 g (20.2 mmol) $NaOAc \cdot 3\ H_2O$ were dissolved in 30 ml methanol and heated to reflux. Then 0.8 ml (9.7 mmol) pyridine were added to the stirred reaction mixture and subsequently 5 ml (58 mmol) 35 m% hydrogen peroxide solution were added dropwise using a dropping funnel over a period of 10 minutes. After 4h, the reaction mixture was cooled to room temperature. The aqueous phase was extracted with dichloromethane (3x 20 ml). The combined organic phase was dried over anhydrous $MgSO_4$ and filtered through a plug of celite. Evaporation of dichloromethane gave a olive green solid. Further purification was done by column chromatography (silica gel 60, gradient CH_2Cl_2 → CH_2Cl_2 : MeOH (95 : 5, *V* : *V*)) to yield pure $Co_4O_4(OAc)_4Py_4$ **I** as green crystalline solid. Yield: 1.50 g (1.8 mmol, 73%).

Suitable crystals for single crystal analysis were obtained by vapour diffusion of diethyl ether into a concentrated solution of **I** in acetonitrile.

^{1}H-NMR (300.13 MHz, acetornitrile-d3): δ = 8.37 (dd, J = 6.4, 1.4 Hz, 8H), 7.58 (tt, J = 7.6, 1.6 Hz, 4H), 7.09 (m, 8H), 1.98 (s, 12H) ppm.
^{13}C (75.47 MHz, acetornitrile-d3): δ = 186.1, 153.3, 138.2, 124.6, 26.6 ppm.
^{59}Co (94.94 MHz, acetornitrile-d3): δ = 11760 ppm.

^{1}H-NMR (400.13 MHz, D_2O): δ = 8.31 (m, 8H), 7.82 (m, 4H), 7.32 (m, 8H), 2.18 (s, 12H) ppm.
^{13}C (100.61 MHz, D_2O): δ = 188.9, 152.1, 139.0, 124.9, 25.7 ppm.
^{59}Co (94.94 MHz, D_2O): δ = 12066 ppm.

^{1}H-NMR (300.13 MHz, MeOH-d4): δ = 8.43 (m, 8H), 7.67 (tt, J = 7.6, 1.4 Hz, 4H), 7.19 (m, 8H), 2.10 (s, 12H) ppm.

$Co_4O_4(OAc)_4\{^{15}N\}Py_4$ **{^{15}N}I**

The synthesis was done as described for the non-labelled cubane replacing pyridine with ^{15}N pyridine.

Yield: 484 mg (0.57 mmol, 77%)

Further purification was achieved by layering a solution of 100 mg **{^{15}N}I** in 20 ml CH_2Cl_2 with 10 ml *n*-hexane. After slow evaporation overnight the crystal formed were isolated, washed with *n*-hexane and dried. Typical yield: 50 mg needle-shaped crystals which were used for NMR-experiments.

^{1}H-NMR (400.13 MHz, acetornitrile-d3): δ = 8.37 (m, 8H), 7.58 (m, 4H), 7.09 (m, 8H), 1.99 (s, 12H) ppm.
^{15}N (40.54 MHz, acetornitrile-d3): δ = 244.6 ppm
^{59}Co (94.94 MHz, acetornitrile-d3): δ = 11761 ppm.

^{1}H-NMR (400.13 MHz, D_2O): δ = 8.31 (m, 8H), 7.82 (m, 4H), 7.32 (m, 8H), 2.18 (s, 12H) ppm.
^{15}N (40.54 MHz, D_2O): δ = 233.3 ppm
^{59}Co (94.94 MHz, D_2O): δ = 12068 ppm.

^{1}H-NMR (399.60 MHz, CD_2Cl_2): δ = 8.46 (m, 8H), 7.50 (m, 4H), 7.02 (m, 8H), 2.04 (s, 12H) ppm.
^{13}C (100.47 MHz, CD_2Cl_2): δ = 186.4, 153.0, 137.3, 123.8, 26.9 ppm.
^{15}N (40.49 MHz, CD_2Cl_2): δ = 243.3 ppm
^{59}Co (93.78 MHz, CD_2Cl_2): δ = 11772 ppm.

3. Synthesis of Co_4TPT

The synthesis was done according to a modified literature procedure:[4]

50.6 mg (59 µmol) $Co_4O_4(OAc)_4Py_4$ **I** and 25.6 mg (79 µmol) 2,4,6-tri(4-pyridyl)-1,3,5-triazine (TPT) were placed in a 20 ml quartz ampule. 8 ml of benzonitrile were added, the suspension was ultrasonicated for 10 min and the suspension degassed by 3 freeze-pump-thaw cycles. The ampule was sealed under vacuum and placed in an oven preheated to 100 °C. After four days, the ampule was removed from the oven, opened (after cooling to room temperature), the red gel was transferred to a Soxhlet fumble and purified by Soxhlet extraction with methanol (24 h). Drying under reduced pressure (80°C) gave Co_4TPT as dark red solid. Yield: 40.1 mg (42 µmol, 71 %).

CHN analysis, expected values: C: 40.36 H: 2.96 N:11.77
experimental results: C: 35.62(4) H: 4.40(3) N: 10.49(4)
C:N molar ratio: 3.96(1) expected 4.00

4. Additional Characterisation

To rule out the impact of scalar coupling between the central Co atoms and the surrounding quadrupolar N ligand of pyridine, the molecular complex was analysed both using pyridine with ^{15}N in natural abundance (0.37%) in $Co_4O_4(OAc)_4Py_4$ and enriched with ^{15}N in $Co_4O_4(OAc)_4\{^{15}N\}Py_4$. For ligand atoms with non-zero spin scalar coupling can contribute to line broadening. While in $Co_4O_4(OAc)_4Py_4$ it is supposed that no scalar coupling is observed due to the quadrupolar nature of ^{14}N (99.63% natural abundance) causing quadrupolar relaxation, in $Co_4O_4(OAc)_4\{^{15}N\}Py_4$ scalar coupling between ^{59}Co and ^{15}N might contribute to line-broadening. However, when dissolved in D_2O, the ^{59}Co NMR spectra of both complexes show similar linewidth (Figure S1). Thus, scalar coupling between ^{59}Co and ^{15}N does not significantly contribute to line-broadening. The impact of scalar coupling between ^{59}Co and ^{17}O, the only NMR active nuclei of oxygen, can be neglected due to the low natural abundance (0.038%) and the quadrupolar nature of ^{17}O (spin of 5/2).[5]

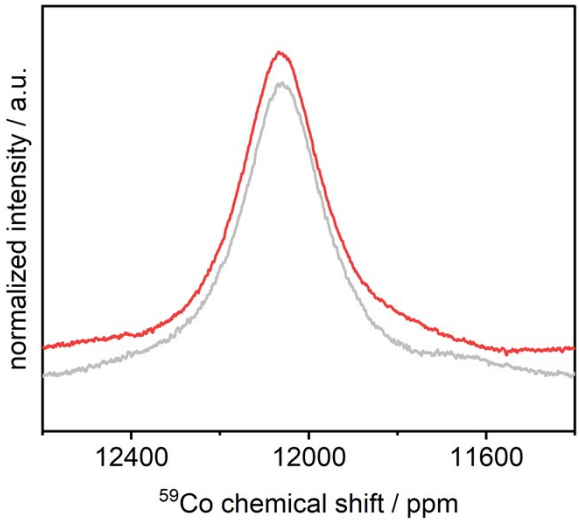

Figure S1. Comparison of ^{59}Co NMR spectrum of $Co_4O_4(OAc)_4Py_4$ (grey) and $Co_4O_4(OAc)_4Py_4$ (red) dissolved in D_2O.

5. Solid-state NMR spectroscopy

5.1. ^{15}N NMR spectroscopy

Solid-state ^{15}N NMR measurements were performed on an Infinity$_{plus}$ spectrometer system (Agilent) operated at 7 T, equipped with a variable-temperature Chemagnetics-Varian 6 mm pencil CPMAS probe. ^{15}N{^{1}H} static and MAS CP NMR spectra were recorded using a 90° pulse length of 5.0 µs. The cross-polarization contact times and relaxation delays were 3 ms and 10 s. The spectra were indirectly referenced to CH_3NO_2 using solid $^{15}NH_4Cl$ (δ = −341.3 ppm). To convert these values to the liquid ammonia scale, 380.6 ppm must be added to them. All ^{15}N chemical shifts are reported with respect to liquid NH_3. The numerical NMR parameters have been extracted from the experimentally obtained spectra using the WSolids1 program package,[6] DMFit and ssNake.[7,8]

Table S 1: Overview of experimental ^{15}N NMR chemical shift tensor (δ_{ref}($^{15}NH_3$ liq.) = 0 ppm).

material / conditions	δ_{iso} / ppm	δ_t / ppm	δ_r / ppm	$\delta_\perp$ / ppm
{^{15}N}-pyridine in D_2O	297			
$Co_4O_4(OAc)_4${^{15}N}Py_4 in D_2O	233			
$Co_4O_4(OAc)_4${^{15}N}Py_4 polycrystalline (MAS)	259(2) 248(2) 239(3)	465(5)	405(5)	-54(1)

5.2. DFT calculations

The Gaussian 09.D.01 program package was used for geometry optimizations and NMR calculations. The TPSSH[9] and ωB97XD[10] DFT hybrid functional and the def2tzvp and def2qzvp[11] basis sets were used. Geometry optimization was done at the very tight convergence criteria. The atom positions obtained from geometry optimisation of $Co_4O_4OAc_4Py_4$ (*Pnnm*, see section 6), $Co_4O_4OAc_4Py_4$ (chloroform solvate, *Pnma*, CCDC 1280106[12], hydrogen positions were optimized using the ωB97XD/def2tzvp approximation) and pyridine are provided in **Table S2**, **Table S3** and **Table S4** respectively. The chloroform solvate of $Co_4O_4OAc_4Py_4$ was used as a reference system in which slightly longer N···Co distances have been reported (**Table S5** - **Table S8**), to evaluate the impact of N···Co distances on the calculated ^{15}N chemical shift.

NMR calculations were carried out using the GIAO approach. All calculations were done using the PCM approximation with water as the solvent. This choice is arbitrary. The outcomes of the PCM approximation are not very sensitive to the value of the dielectric constant.[13] However, this correction is necessary in order to at least approximately consider the effect of the crystal field.

The chemical shift is a relative value. It is calculated based on the absolute shielding of the nucleus in the molecule of interest, σ, and in a reference compound, σ^{ref}. With a high level of accuracy: $\delta \approx \sigma^{ref} - \sigma$.[14–16] The numerical value of σ^{ref} depends on both the DFT functional and the basis set used. For the ωB97XD/def2tzvp and ωB97XD/def2qzvp approximations these values in the CH_3NO_2 chemical shift scale are: σ^{ref} (^{15}N, CH_3NO_2, ωB97XD/def2tzvp) = −143±3 ppm and σ^{ref} (^{15}N, CH_3NO_2, ωB97XD/def2qzvp) = −148±3 ppm.[17] To convert these values to the NH_3 chemical shift scale, 380.6 ppm must be added to them. Thus: σ^{ref} (^{15}N, NH_3, ωB97XD/def2tzvp) = 238±3 ppm and σ^{ref} (^{15}N, NH_3, ωB97XD/def2qzvp) = 233±3 ppm.

For elements beyond the third row of the periodic table, corrections for relativistic effects are necessary when calculating NMR parameters. Such corrections may be necessary even for light atoms due to the shielding effect of a neighboring heavy atom. Nevertheless, in coordination complexes involving pyridine, the heavy-atom effect on the ^{15}N shielding tensor is small, and the primary contribution to the calculation error arises from inaccuracies in determining the molecular structure.[18]

Table S2. DFT optimized atomic coordinates of $Co_4O_4(OAc_4)Py_4$

Atom	x	y	z	Atom	x	y	z
N	5.99027	11.81245	8.43345	H	8.92723	7.34122	9.97901
N	5.99027	11.81245	5.08475	H	8.92723	7.34122	3.53919
N	5.30759	5.91912	6.7591	C	1.57721	10.72812	3.31984
N	2.28673	7.16314	6.7591	C	1.57721	10.72812	10.19836
Co	5.22463	10.0194	8.17247	H	1.09768	11.60158	3.72856
Co	5.22463	10.0194	5.34573	H	1.09768	11.60158	9.78964
Co	5.84912	7.8034	6.7591	H	2.09248	10.99317	2.412
Co	3.23423	8.87308	6.7591	H	2.09248	10.99317	11.1062
O	4.51494	8.32073	7.97907	H	0.8346	9.97817	3.10529
O	4.51494	8.32073	5.53913	H	0.8346	9.97817	10.41291
O	6.36514	9.60058	6.7591	C	4.62259	3.96836	5.57819
O	4.10299	10.53942	6.7591	C	4.62259	3.96836	7.94001
O	6.46011	9.28451	9.4833	H	4.44634	3.47973	4.62789
O	6.46011	9.28451	4.0349	H	4.44634	3.47973	8.89031
O	7.12272	7.49866	8.2394	C	5.75442	14.15967	8.85026
O	7.12272	7.49866	5.2788	C	5.75442	14.15967	4.66794
O	3.79353	10.41233	4.06704	H	5.10798	14.99954	9.07302
O	3.79353	10.41233	9.45116	H	5.10798	14.99954	4.44518
O	2.10086	9.56822	5.31401	C	7.31638	11.97191	8.36153
O	2.10086	9.56822	8.20419	C	7.31638	11.97191	5.15667
C	7.13292	8.23882	9.27386	H	7.94446	11.10721	8.18635
C	7.13292	8.23882	4.24434	H	7.94446	11.10721	5.33185
C	2.57115	10.18177	4.32334	C	7.90223	13.21201	8.5053
C	2.57115	10.18177	9.19486	C	7.90223	13.21201	5.0129
C	4.39705	3.29588	6.7591	H	8.97768	13.31631	8.43164
H	4.05269	2.26909	6.7591	H	8.97768	13.31631	5.08656
C	5.07517	5.27037	5.61894	C	7.11258	14.32221	8.74384
C	5.07517	5.27037	7.89926	C	7.11258	14.32221	4.77436
H	5.24919	5.78789	4.68364	H	7.55902	15.30372	8.84495
H	5.24919	5.78789	8.83456	H	7.55902	15.30372	4.67325
C	5.23269	12.88424	8.66353	C	0.81974	4.82592	6.7591
C	5.23269	12.88424	4.85467	H	0.20841	3.93196	6.7591
H	4.15823	12.75576	8.70724	C	1.94191	6.57445	5.62694
H	4.15823	12.75576	4.81096	C	1.94191	6.57445	7.89126
C	8.05611	7.8208	10.39264	H	2.24323	7.03127	4.69238
C	8.05611	7.8208	3.12556	H	2.24323	7.03127	8.82582
H	8.3569	8.68966	10.95347	C	1.21675	5.40649	7.93304
H	8.3569	8.68966	2.56473	C	1.21675	5.40649	5.58516
H	7.54288	7.13326	11.04365	H	0.96319	4.95208	8.88283
H	7.54288	7.13326	2.47455	H	0.96319	4.95208	4.63537

Table S3. DFT optimized atomic coordinates of $Co_4O_4(OAc_4)Py_4$ chloroform solvate (CCDC 1280106,[12] *Pnma* (62), **Cell**: a 10.181(4)Å b 21.655(2)Å c 27.407(6)Å)

Atom	x	y	z
Co	0.916052	-1.409742	-0.003225
Co	-0.895596	-0.000034	-1.396217
Co	-0.863785	-0.000035	1.421579
O	-0.928388	-1.191034	0.034547
O	0.928903	-0.000042	-1.293835
O	1.01448	-0.000043	1.230096
O	0.649596	-2.717741	-1.408585
O	-0.718394	-1.446535	-2.714126
O	0.748975	-2.683042	1.458396
O	-0.652581	-1.474736	2.731036
N	2.865216	-1.686951	-0.039601
N	-2.857908	-0.000026	-1.581244
N	-2.827447	-0.000027	1.677564
C	-0.0542	-2.522838	-2.468189
C	-0.171862	-3.646737	-3.425228
C	0.023058	-2.516339	2.469566
C	-0.076688	-3.599039	3.481066
C	3.582261	-1.645754	1.120258
C	4.941365	-1.82116	1.142083
C	5.564477	-1.996562	-0.068556
C	4.887482	-2.074559	-1.212918
C	3.536106	-1.864453	-1.196185
C	-3.550223	-1.134723	-1.672361
C	-4.900668	-1.180117	-1.911626
C	-5.500467	-0.000014	-2.018405
C	-3.53339	-1.178024	1.714163
C	-4.863639	-1.245118	1.912369
C	-5.544321	-0.000015	1.966462
O	-0.928378	1.191066	0.034547
Co	0.916064	1.409758	-0.003224
O	0.649619	2.717759	-1.408583
C	-0.054178	2.522862	-2.468187
O	-0.718381	1.446565	-2.714125
O	-0.652569	1.474764	2.731036
C	0.023079	2.516361	2.469567
O	0.748998	2.683058	1.458398
N	2.86523	1.686949	-0.0396
C	3.582275	1.645746	1.120258
C	4.941381	1.82114	1.142084
C	5.564494	1.996538	-0.068555

Atom	x	y	z
C	4.8875	2.074541	-1.212917
C	3.536122	1.864447	-1.196184
C	-0.076657	3.599061	3.481068
C	-4.863628	1.245182	1.91237
C	-3.53338	1.178076	1.714163
C	-4.900658	1.180183	-1.911626
C	-3.550213	1.134777	-1.672361
C	-0.171831	3.646763	-3.425226
H	-1.080809	4.025333	3.439893
H	0.649215	4.389108	3.301452
H	0.062582	3.185979	4.479108
H	2.929728	1.862934	-2.090298
H	5.389145	2.231917	-2.1578
H	6.642461	2.11655	-0.082157
H	5.489547	1.775372	2.071313
H	2.994217	1.472219	2.009771
H	0.649226	-4.389056	3.301487
H	0.062478	-3.185952	4.479114
H	2.994204	-1.472221	2.009769
H	5.489532	-1.775397	2.071312
H	6.642443	-2.116583	-0.082159
H	5.389126	-2.231938	-2.157801
H	2.929712	-1.862932	-2.090298
H	-2.962473	-2.036656	-1.562294
H	-5.421529	-2.121899	-1.98974
H	-6.572055	-0.000009	-2.20813
H	-2.913209	-2.059035	1.62054
H	-5.395095	-2.183172	1.957494
H	-6.620454	-0.000011	2.091872
H	-2.913151	2.059048	1.620533
H	-5.395107	2.183222	1.957495
H	-0.361684	-3.283115	-4.432773
H	0.719147	-4.270369	-3.406631
H	-1.023039	-4.260556	-3.121058
H	-1.080819	-4.025355	3.439833
H	-2.962415	2.036673	-1.562281
H	-5.421544	2.12195	-1.989741
H	-0.361631	3.28314	-4.432775
H	0.719172	4.270404	-3.406612
H	-1.023019	4.260575	-3.121073

Table S4. DFT optimized atomic coordinates of Py.

Atom	x	y	z
C	1.142559	0.719172	-0.000001
C	1.195157	-0.670484	0
C	-0.000013	-1.380496	-0.000001
C	-1.195168	-0.670464	0
C	-1.142546	0.719193	-0.000001
H	2.057722	1.301539	0.000003
H	2.150471	-1.178513	0.000002
H	-0.000021	-2.463056	0.000001
H	-2.150495	-1.178472	0.000002
H	-2.057699	1.301575	0.000003
N	0.000013	1.416486	0

Table S5. ^{15}N NMR chemical shift tensors of the selected structures calculated at the GIAO wB97XD/def2tzvp PCM = water approximation (δ_{ref}($^{15}NH_3$ liq.) = 0 ppm).

structure	N···Co distance, Å	δ_{iso}, ppm	δ_t, ppm	δ_r, ppm	$\delta_\perp$, ppm
$Co_4O_4(OAc_4)Py_4$ (chloroform solvate CCDC 1280106[12])	1.96911	284	473	450	−72
	1.97102	269	459	426	−77
	1.98028	284	469	447	−63
	1.96911	284	473	450	−72
$Co_4O_4(OAc_4)Py_4$	1.96707	270	450	438	−78
	1.96707	270	450	438	−78
	1.96055	265	446	431	−80
	1.95490	260	437	428	−85
Pyridine		321	605	419	−61

Table S6. ^{15}N NMR shielding tensors of the selected structures calculated at the GIAO wB97XD/def2tzvp PCM = water approximation (δ_{ref}($^{15}NH_3$ liq.) = 0 ppm).

structure	N···Co distance, Å	σ_{iso}, ppm	σ_t, ppm	σ_r, ppm	$\sigma_\perp$, ppm
$Co_4O_4(OAc_4)Py_4$ (chloroform solvate CCDC 1280106[12])	1.96911	−45.7	−235.0	−212.2	310.0
	1.97102	−31.3	−221.3	−187.6	315.1
	1.98028	−46.1	−230.6	−209.0	301.3
	1.96911	−45.7	−235.0	−212.2	310.0
$Co_4O_4(OAc_4)Py_4$	1.96707	−32.0	−211.9	−200.0	315.8
	1.96707	−32.0	−211.9	−200.0	315.8
	1.96055	−27.4	−207.6	−192.6	317.9
	1.95490	−22.0	−199.2	−189.7	323.0
Pyridine		−82.9	−366.7	−180.9	298.8

Table S7. ^{15}N NMR chemical shift tensors of the selected structures calculated at the GIAO wB97XD/def2qzvp PCM = water approximation ($\delta_{ref}(^{15}NH_3$ liq.) = 0 ppm).

structure	N···Co distance, Å	δ_{iso}, ppm	δ_t, ppm	δ_r, ppm	$\delta_\perp$, ppm
$Co_4O_4(OAc_4)Py_4$ (chloroform solvate CCDC 1280106[12])	1.96911	286	476	454	−72
	1.97102	271	462	429	−78
	1.98028	286	471	449	−62
	1.96911	286	476	454	−72
$Co_4O_4(OAc_4)Py_4$	1.96707	270	454	441	−84
	1.96707	270	454	441	−84
	1.96055	266	480	436	−86
	1.95490	260	439	433	−91
Pyridine		320	605	420	−64

Table S8. ^{15}N NMR shielding tensors of the selected structures calculated at the GIAO wB97XD/def2qzvp PCM = water approximation ($\delta_{ref}(^{15}NH_3$ liq.) = 0 ppm).

structure	N···Co distance, Å	σ_{iso}, ppm	σ_t, ppm	σ_r, ppm	$\sigma_\perp$, ppm
$Co_4O_4(OAc_4)Py_4$ (chloroform solvate CCDC 1280106[12])	1.96911	−52.8	−242.5	−220.8	304.7
	1.97102	−38.2	−229.0	−196.1	310.6
	1.98028	−53.2	−238.0	−216.4	294.7
	1.96911	−52.8	−242.5	−220.8	304.7
$Co_4O_4(OAc_4)Py_4$	1.96707	−37.2	−220.7	−207.9	317.1
	1.96707	−37.2	−220.7	−207.9	317.1
	1.96055	−32.6	−214.0	−203.0	319.1
	1.95490	−27.1	−205.8	−199.7	324.0
Pyridine		−87.4	−371.7	−187.3	296.8

5.3. Fast MAS NMR spectroscopy

Solid-state NMR spectra were acquired using JEOL 600 MHz spectrometer (14.09 T) under MAS conditions with rotation rate of 70.0 and 62.5 kHz MAS (1.0 mm zirconia rotor) and Bruker Avance III 800 MHz (18.79 T) at 50 and 55 kHz MAS (1.3 mm zirconia rotor). Magic angle was calibrated using KBr external sample. All experiments were performed at room temperature of approximately 23˚C without temperature regulation.

The ^{1}H-^{13}C and ^{1}H-^{14}N correlation spectra were acquired using double cross-polarisation (DCP) experiment and TRAPDOR-HMQC,[19] respectively, after 0.8 µs (90˚) ^{1}H excitation pulse. In the DCP ^{1}H-^{13}C we used 1.0 and 0.3 ms forward and backward CP mixing time, respectively. In the TRAPDOR-HMQC coherence transfer was assured by two 2ms high-power ^{14}N pulses on resonance with 1st rotation sideband. The ^{1}H and ^{13}C 1D spectra were acquired using spin-echo and CPMAS experiments, respectively. Repetition time of 2.0 and 0.5 s (1.5x T_1) was used for $Co_4O_4(OAc)_4Py_4$ and Co_4TPT, respectively.

The ^{59}Co spectra were acquired using single pulse experiment (pulse duration of 2.5 and 0.35 µs for 600 and 800MHz spectrometer, resp.) with direct FID detection. Quadrupolar coupling (approx. 40 MHz) constant as well as pure isotropic ^{59}Co chemical shift were obtained from linear dependence of the position of the isotropic-signal centre of gravity on the square of ^{59}Co resonance frequency.[20] The isotropic signal was identified by measurement at different MAS rates. Zero asymmetry was assumed. Repetition delay was set to 0.5 s.

Chemical shifts were referenced using external sample of alanine (^{1}H at 1.237 ppm), adamantane (^{13}C at 37.8 ppm) and solution of $Co(acac)_3$ in chloroform (^{59}Co at 12500 ppm with respect to saturated $K_3[Co(CN)_6]$ in D_2O),[21] the ^{14}N spectra were referenced with respect to liquid NH_3 by unified scale as recommended by IUPAC[1,2]

In case of ^{14}N/^{15}N MAS NMR spectra of $Co_4O_4(OAc)_4Py_4$, the comparison of ^{15}N chemical shift ($\delta_{15N} = 248.6$ ppm, mean value from Table S 1) and observed centre of gravity of the signal in the ^{14}N projection of the TRAPDOR-HMQC spectra $\delta_{14N} = 576$ ppm (Figure 2D) gives second-order quadrupolar shift δ^{Q}_{iso}:

$$\delta^{Q}_{iso} = \delta_{14N} - \delta_{15N} = 327\ ppm$$

which can be used for calculation of the quadrupolar product P_Q:

$$P_Q = \nu^{0}_{14N}\sqrt{10^{-6} \times \frac{40}{3}\delta^{Q}_{iso}} = 2.86\ MHz,$$

where $\nu^{0}_{14N} = 43.354$ MHz corresponds to Larmor frequency of ^{14}N nucleus. Under an assumption of zero quadrupolar-coupling asymmetry, the value of the quadrupolar product is equivalent to the coupling constant C_Q.[22]

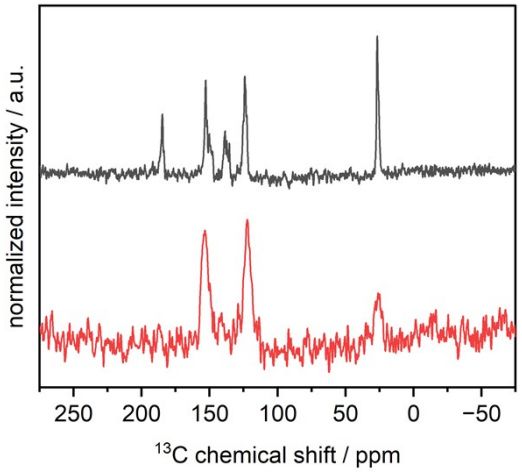

Figure S2. Solid-state ^{13}C CPMAS spectra of $Co_4O_4(OAc)_4Py_4$ (grey) and Co_4TPT (red) acquired at B_0 14.09 T under 62.5 and 70 kHz, respectively.

6. Photocatalytic OER and catalyst characterization

OER experiments were carried out in a home built 48 ml front irradiation quartz reactor,[23,24] equipped with a stirring bar and connected to a FireSting-O_2 Fiber-Optic Oxygen Meter (Robust Oxygen Probe OXROB10, both PyroScience GmbH) to measure the oxygen content in the gas phase. For a typical experiment using Co-TPT, ~10 mg of the solid catalyst were placed inside the reactor. The reactor was carefully evacuated and back-filled with Ar to remove air. Under a counterflow of Ar, 20 ml of a fresh, deaerated solution containing 5 mM of $Na_2S_2O_8$ and 1 mM $Ru(bpy)_3Cl_2$ in a borate buffer (0.05 M, adjusted to pH 8 with sulfuric acid) were added. The reactor was sealed with rubber stoppers. The measurement was started under dark conditions and after approx. 180 s the reactor was irradiated using a 100 W Xe lamp (Siemens) equipped with a 420 nm bandpass filter, with a fixed distance of 10 cm between the light source and the reactor.

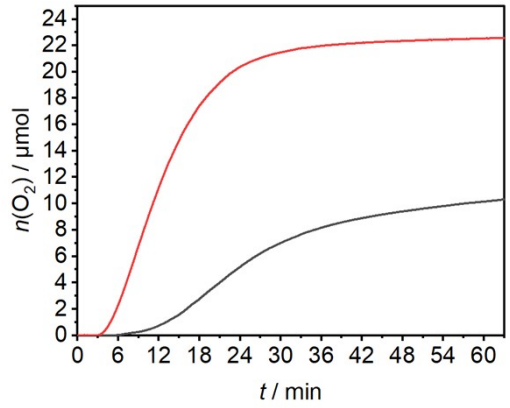

Figure S3. Comparison of OER activity for of $Co_4O_4OAc_4Py_4$ (dark grey, 12 µmol) fresh Co-TPT (red, 8.7 µmol) in the presence of $Ru(bpy)_3Cl_2$ (21 µmol) as a photosensitizer in aqueous borate buffer (pH 8, ~0.1 mmol $Na_2S_2O_8$), 1 h.

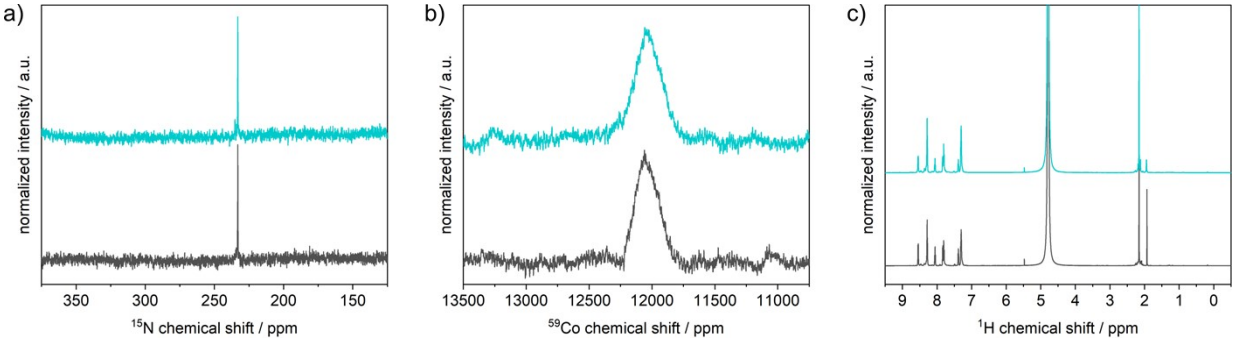

Figure S4. ^{15}N, ^{59}Co and ^{1}H NMR spectra of a solution of $Co_4O_4(OAc)_4\{^{15}N\}Py_4$ in D_2O (0.05M Na2B2O7, adjusted with DCl to pH 7.9) containing 5 mM $Ru(bpy)_3Cl_2$ and 30 mM $Na_2S_2O_8$ before (grey) and after photocatalysis (cyan, irradiation for 1h with a 100 W lamp).

Table S9. Overview of catalytic activity and comparison to literature. For each standard experiment at least two independent catalytic experiments were performed.

material	n_{cubane} / µmol	n_{O2} / µmol	yield / %	*TON*	*TOF*	*R* / µmol/g/s	ref
$Co_4O_4OAc_4Py_4$	12.5±0.1	14.7±2.5	27±4	1.2±0.2	$(1.2\pm0.2)\cdot10^{-3}$	1.5±0.1	this work
	0.332			40±2	$2.0\cdot10^{-2}$ [b]	--	[25] [c]
	1.08	2.5	7	2.3	$0.2\cdot10^{-3}$		[26] [d]
	0.036	5.0	100	140	$1.0\cdot10^{-3}$		[27] [e]
	0.02 – 0.2				$\sim3\cdot10^{-2}$		[28] [f]
CoTPT (av)	8.7±0.3	20.9±0.9	37±3	2.4±0.1	$(3.2\pm0.1)\cdot10^{-3}$	2.8±0.2	this work
1st cycle [a]	8.4	20.0±0.9	33±3	2.4±0.1	$(3.5\pm0.1)\cdot10^{-3}$	3.0±0.2	this work
2nd cycle [a]	8.4	15.9±0.7	32±3	1.9±0.1	$(3.0\pm0.1)\cdot10^{-3}$	3.0±0.2	this work
3rd cycle [a]	8.4	24.1±1.1	34±3	2.9±0.1	$(3.4\pm0.1)\cdot10^{-3}$	3.0±0.2	this work
4th cycle [a]	8.4	22.0±1.0	37±3	2.6±0.1	$(3.4\pm0.1)\cdot10^{-3}$	2.9±0.2	this work

[a] for estimation of the error on recycling experiments the relative error η observed for CoTPT, was used to calculate the error bar for each point, even if this procedure overestimates the errors for some experimen[29,30]

[b] from dissolved oxygen determined using a Clark electrode; [c] pH 7, carbonate buffer, 250 W lamp; [d] pH 8, borate buffer, 450 nm LEDs; [e] pH 8, borate buffer, acetonitrile : water (1:1), 50 W halogen lamp; [f] pH 8, borate buffer LEDs

For recycling experiments, the solid catalyst was allowed to settle. Under a counterflow of Ar, the supernatant was carefully removed with a syringe. The supernatant was evaporated to dryness and redissolved in deionised water for ICP analysis of the amount of Co. 20 ml of a fresh, deaerated solution containing 5 mM of $Na_2S_2O_8$ and 1 mM $Ru(bpy)_3Cl_2$ in a borate buffer (0.05 M, adjusted to pH 8 with sulfuric acid) were added, and the next cycle of OER was conducted. Over this series of 4 cycles, the TOF varied only slightly (Figure S5). To confirm the heterogeneous nature of the catalyst the liquid supernatant after each cycle was analysed by inductively coupled plasma optical emission spectroscopy. After each cycle small amounts of Co are leached in the supernatant (**Table S10**). Note that traces of decomposed cubane, their presence depending on the reaction conditions, have been reported to be catalytically inactive.[26] In line with those results, the IR spectrum of the spent catalyst confirms the stable nature of the framework, i.e. the cubane TPT coordinative bonds (Figure S6). After four cycles of catalysis the acetate ligands are completely replaced most likely by water and OH groups.[4,31] The absence of any additional bands in the 1200 – 1000 cm^{-1} and 650 – 550 cm^{-1} regions rule out the coordination of borate or sulfate (from $S_2O_8^{2-}$) to the Co centres. This is further confirmed by the ^{59}Co NMR investigations of the homogeneous complex, where we did not observe any indication of such coordination. The stability of the Co-cubane core after catalysis is further evidenced by the characteristic bands around 670, 640 ($\nu_s(Co-\mu_3O)$ and 580 cm^{-1}, which has been defined as the cubane's markers.[3]

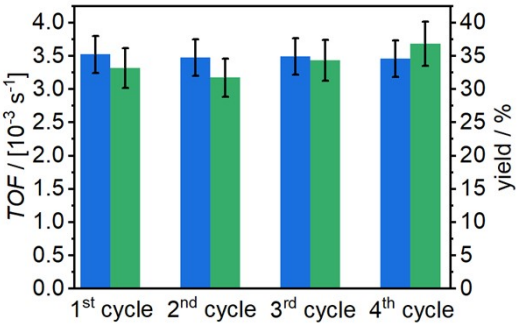

Figure S5. Catalytic activity over four cycles of catalysis using Co-TPT (~8.4 µmol) in the presence of $Ru(bpy)_3Cl_2$ (21 µmol) as a photosensitizer in aqueous borate buffer (pH 8, ~0.1 mmol $Na_2S_2O_8$), 1 h. After each run, the solid was isolated by sedimentation and reused with a fresh solution of buffer solution containing $Ru(bpy)_3Cl_2$ and $Na_2S_2O_8$.

Table S10. Overview of leached amount of Co after each cycle into the supernatant as determined by ICP OES.

	after 1st run	after 2nd run	after 3rd run	after 4th run
β_{Co} / ppm	3.6	3.5	4.2	2.5

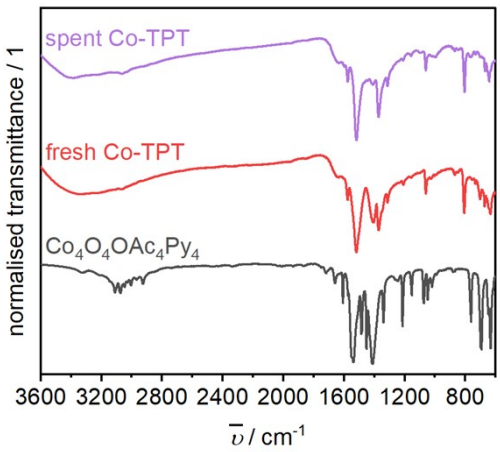

Figure S6. IR spectra of $Co_4O_4(OAc)_4Py_4$ (black), fresh Co-TPT (red) and spent Co-TPT after four cycles of photocatalysis (purple).

7. Single crystal data

Summary of structure solution

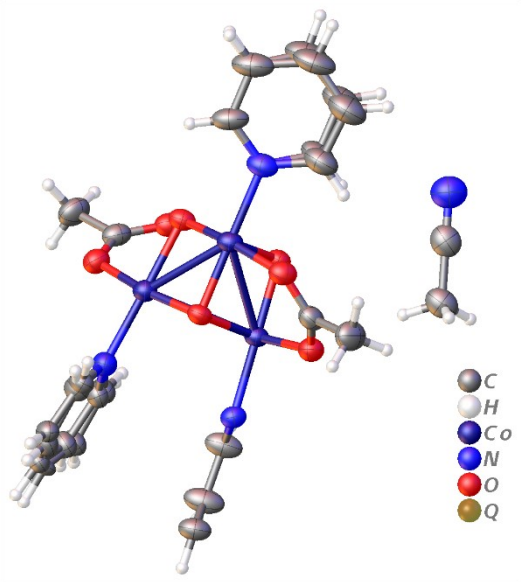

Compound	$Co_4O_4(OAc)_4Py_4$
Formula	$C_{30}H_{35}Co_4N_5O_{12}$
$D_{calc.}$/ g cm^{-3}	1.615
μ/mm^{-1}	14.459
Formula Weight	893.372
Colour	clear dark green
Shape	needle-shaped
Size/mm^3	0.25×0.04×0.04
T/K	123.00(10)
Crystal System	orthorhombic
Space Group	Pnnm
a/Å	19.6668(2)
b/Å	13.8232(1)
c/Å	13.5182(1)
α/°	90
β/°	90
γ/°	90
V/Å^3	3675.03(5)
Z	4
Z'	0.5
Wavelength/Å	1.54184
Radiation type	Cu Kα
Q_{min}/°	3.91
Q_{max}/°	75.92
Measured Refl's.	60800
Indep't Refl's	3938
Refl's I≥2 s(I)	3602
R_{int}	0.0438
Parameters	341
Restraints	416
Largest Peak	0.5862
Deepest Hole	-0.2986
GooF	1.0400
wR_2 (all data)	0.0914
wR_2	0.0893
R_1 (all data)	0.0351
R_1	0.0321

Single clear dark green needle-shaped crystals of **$Co_4O_4OAc_4Py_4$** were used as supplied. A suitable crystal with dimensions 0.25 × 0.04 × 0.04 mm^3 was selected and mounted on a XtaLAB Synergy R, DW system, HyPix-Arc 150 diffractometer. The crystal was kept at a steady *T* = 123.00(10) K during data collection. The structure was solved with the ShelXT 2018/2,[32] solution program using iterative methods and by using Olex2 1.5-alpha as the graphical interface.[33] The model was refined with olex2.refine 1.5-alpha using full matrix least squares minimisation on ***F*²**.[34]

The unit cell was refined using CrysAlisPro 1.171.43.17a[35] on 30562 reflections, 50% of the observed reflections.
Data reduction, scaling and absorption corrections were performed using CrysAlisPro 1.171.43.17a (Rigaku OD, 2022). The final completeness is 99.97 % out to 75.92° in *Θ*. A gaussian absorption correction was performed using CrysAlisPro 1.171.43.17a. Numerical absorption correction based on gaussian integration over a multifaceted crystal model Empirical absorption correction using spherical harmonics, implemented in SCALE3 ABSPACK scaling algorithm. The absorption coefficient *μ* of this material is 14.459 mm^{-1} at this wavelength (*λ* = 1.54184Å) and the minimum and maximum transmissions are 0.152 and 0.845.
The structure was solved and the space group *Pnnm* (# 58) determined by the ShelXT 2018/2[32] structure solution program using iterative methods and refined by full matrix least squares minimisation on F^2 using version of olex2.refine 1.5-alpha.[34] All non-hydrogen atoms were refined anisotropically. Hydrogen atom positions were calculated geometrically and refined using the riding model. Hydrogen atom positions were calculated geometrically and refined using the riding model.
_exptl_absorpt_process_details: CrysAlisPro 1.171.43.17a. Numerical absorption correction based on gaussian integration multifaceted crystal model. Empirical absorption correction using spherical harmonics, implemented in SCALE3 ABSPACK scaling algorithm.
The value of Z' is 0.5. This means that only half of the formula unit is present in the asymmetric unit, with the other half consisting of symmetry equivalent atoms.

A Hirshfeld-Atom-Refinement (HAR) using the software *NoSpherA2*[36] was used to obtain non-spherical atomic formfactors for all but hydrogen atoms in the structure. Modelling hydrogen atoms anistropically and with a free distance was not possible for a converged model. We attribute this to the disorder and the coordinated pyridyl groups. Generally, HAR improved the agreement between the measured and calculated data by 0.62% in R1 and 1.35% in wR2, substantially improving the model for this metalorganic compound.

A solvent mask was calculated, and 66 electrons were found in a volume of 216 Å^3, which were attributed to the presence of approximately one molecule of acetonitrile (88 electrons) per asymmetric unit. The solvent molecule was heavily disordered and could not be modelled properly without inflicting the part of interest in the crystallographic structure.

Table S11. Fractional Atomic Coordinates (×10^4) and Equivalent Isotropic Displacement Parameters (Å^2×10^3) for $Co_4O_4OAc_4Py_4$. U_{eq} is defined as 1/3 of the trace of the orthogonalised U_{ij}.

Atom	x	y	z	U_{eq}
Co^{01}	2656.67(17)	7248.0(2)	6045.8(2)	33.65(11)
Co^{02}	2974.2(2)	5645.0(3)	5000	31.94(12)
Co^{03}	1644.6(2)	6418.7(3)	5000	33.76(12)
O^{004}	2296.0(7)	6017.9(10)	5903.5(10)	33.2(3)
O^{005}	3237.0(10)	6944.7(13)	5000	32.3(4)
O^{006}	2086.4(11)	7623.6(14)	5000	36.3(4)
O^{007}	3285.6(8)	6717.6(10)	7015.0(11)	40.6(3)
O^{008}	3622.5(8)	5424.0(10)	6094.7(11)	40.5(3)
O^{009}	1929.1(8)	7534.6(10)	3008.8(11)	40.8(3)
O^{00A}	1065.9(8)	6920.9(11)	3931.5(12)	42.9(4)
N^{00B}	2697.8(13)	4284.6(17)	5000	34.6(5)
C^{00E}	3625.2(11)	5960.0(15)	6858.8(17)	39.8(5)
C^{00F}	1307.8(12)	7366.7(15)	3197.4(17)	41.7(5)
N^{00G}	5265(2)	8086(3)	5000	70.7(9)
C^{00H}	2236.7(19)	2388(2)	5000	46.7(8)
C^{00I}	5227(2)	7262(3)	5000	54.7(9)
C^{00J}	2581.9(15)	3809.1(17)	4157.0(18)	51.5(6)
C^{00K}	2659.4(16)	9323.8(16)	6411.7(19)	53.4(6)
C^{00L}	4091.9(14)	5657.1(19)	7689(2)	57.3(7)
C^{00M}	5178(2)	6210(3)	5000	55.9(9)
C^{00N}	799.2(14)	7754.4(18)	2459(2)	56.3(7)
C^{00O}	2347.9(17)	2872.4(18)	4127(2)	58.7(7)
C^{00Q}	2930.6(19)	10239.4(19)	6547(2)	67.1(8)
C^{00R}	3701(5)	8726(8)	6011(8)	54.5(18)
C^{00T}	3561(6)	10429(8)	6322(9)	69.1(19)
C^{00W}	3981(5)	9649(6)	6056(8)	66.1(17)
N^{00E}	3045.0(11)	8544.6(13)	6238.0(14)	44.4(4)
C^{4}	3741(5)	8605(6)	6332(7)	58.1(17)
C^{00X}	4053(4)	9485(5)	6505(8)	74.2(17)
C^{00U}	3663(5)	10292(7)	6588(8)	72.1(18)
N^{2}	1165.1(13)	5180.9(19)	5000	42.7(6)
C^{3}	888(9)	4868(11)	5823(10)	41(2)
C^{1}	485(6)	4043(8)	5831(8)	37(2)
C^{5}	384(11)	3531(14)	5000	36(2)
C^{6}	690(8)	3823(11)	4132(10)	43(2)
C^{7}	1080(9)	4658(10)	4152(10)	42(2)
C^{3a}	832(9)	4763(12)	5681(11)	43(2)
C^{1a}	470(7)	3841(10)	5543(10)	44(2)
C^{5a}	448(6)	3442(8)	4775(7)	31(2)
C^{6a}	803(7)	3851(10)	3920(10)	41.3(19)
C^{7a}	1152(9)	4731(11)	4019(11)	41(2)

Table S12. Anisotropic Displacement Parameters (×10^4) for $Co_4O_4OAc_4Py_4$. The anisotropic displacement factor exponent takes the form: $-2\pi^2[h^2a^{*2} \times U_{11} + ... + 2hka^* \times b^* \times U_{12}]$.

Atom	U11	U22	U33	U23	U13	U12
Co01	41.1(2)	25.39(17)	34.43(18)	-2.29(12)	0.14(13)	-1.40(12)
Co02	35.6(2)	24.7(2)	35.4(2)	-1.73(17)	-0	0
Co03	35.4(2)	27.8(2)	38.0(2)	-0.55(17)	-0	0
O004	37.2(7)	26.3(6)	36.1(7)	-5.5(5)	-1.1(6)	1.6(5)
O005	34.2(10)	24.6(9)	38.0(10)	-5.1(8)	-0	0
O006	43.6(11)	27.8(9)	37.5(11)	-5.5(8)	-0	0
O007	47.3(8)	35.0(7)	39.5(8)	-3.4(6)	-4.6(7)	-0.9(6)
O008	39.8(8)	33.7(7)	47.9(8)	-0.4(6)	-2.4(7)	0.5(6)
O009	50.7(9)	33.0(7)	38.7(8)	1.8(6)	-3.2(7)	1.4(6)
O00A	42.8(8)	37.0(8)	48.7(9)	4.0(6)	-3.3(7)	0.1(7)
N00B	39.8(13)	28.8(11)	35.0(12)	2.4(10)	-0	0
C00E	39.4(11)	36.0(10)	43.9(11)	-7.4(9)	-4.8(9)	2.4(9)
C00F	52.0(13)	30.5(10)	42.5(12)	4.8(9)	-6.0(10)	-1.5(9)
N00G	80(2)	61(2)	71(2)	1.3(19)	-0	0
C00H	64(2)	30.3(15)	45.2(18)	-6.0(14)	-0	0
C00I	57(2)	62(2)	44.6(19)	-6.0(17)	-0	0
C00J	83.0(18)	38.6(12)	33.0(11)	-14.5(12)	0.5(11)	-0.3(9)
C00K	83.9(18)	29.0(10)	47.4(13)	1.2(10)	4.1(12)	-0.7(9)
C00L	55.7(15)	51.8(14)	64.6(16)	-0.4(12)	-20.2(13)	-0.1(12)
C00M	63(2)	56(2)	48.6(19)	-12.7(18)	-0	0
C00N	59.8(16)	48.1(13)	60.9(16)	12.6(11)	-13.0(13)	5.5(11)
C00O	98(2)	39.5(13)	38.8(13)	-16.3(13)	2.6(13)	-3.9(10)
C00Q	108(2)	35.4(12)	58.2(16)	-7.2(12)	8.2(14)	-3.0(10)
C00R	64(3)	44(3)	55(4)	-20.0(18)	0(2)	-7(2)
C00T	103(3)	38(3)	66(4)	-19.4(17)	3(2)	-5(2)
C00W	83(3)	50(3)	65(4)	-25.6(17)	2(2)	-7(2)
N00E	59.6(12)	33.6(9)	40.1(10)	-7.5(8)	2.3(9)	-4.0(7)
C4	69(3)	45(3)	60(4)	-19.3(18)	4(2)	-4(2)
C00X	87(3)	57(3)	79(4)	-27.0(19)	-1(2)	-3(2)
C00U	107(4)	41(3)	68(4)	-27(2)	0(2)	-7(2)
N2	36.7(13)	34.8(12)	56.6(15)	-0.6(10)	-0	0
C3	38(4)	32(4)	55(4)	-4(2)	2.2(18)	-0.9(17)
C1	32(4)	28(4)	51(4)	0(2)	3.0(18)	-2.2(16)
C5	28(4)	30(4)	48(5)	-3(2)	-0	0
C6	35(4)	42(3)	52(4)	-7(2)	2.8(17)	-1.6(16)
C7	32(4)	40(3)	55(4)	-4(2)	2.1(18)	-0.6(17)
C3a	38(4)	37(4)	53(4)	-4(2)	2(2)	-2(2)
C1a	35(4)	41(5)	57(5)	-4(3)	2(2)	5(2)
C5a	30(4)	18(3)	44(5)	-7(2)	-2(2)	4(2)
C6a	35(4)	39(3)	50(4)	-9(2)	4(2)	-1(2)
C7a	33(4)	38(4)	53(4)	-6(2)	0(2)	-5(2)

Table S13. Bond Lengths in Å for $Co_4O_4OAc_4Py_4$.

Atom	Atom	Length/Å
Co01	Co011	2.8275(7)
Co01	Co021	2.7016(5)
Co01	Co031	2.6971(5)
Co01	O004	1.8525(13)
Co01	O0051	1.8647(13)
Co01	O0061	1.8778(15)
Co01	O007	1.9452(15)
Co01	O0091	1.9590(15)
Co01	N00E	1.9654(19)
Co02	Co03	2.8251(6)
Co02	O004	1.8806(14)
Co02	O0041	1.8806(14)
Co02	O005	1.8694(18)
Co02	O0081	1.9771(16)
Co02	O008	1.9771(16)
Co02	N00B	1.958(2)
Co03	O004	1.8547(14)
Co03	O0041	1.8547(14)
Co03	O006	1.879(2)
Co03	O00A	1.9656(16)
Co03	O00A1	1.9656(16)
Co03	N2	1.954(3)
O007	C00E	1.260(3)
O008	C00E	1.271(3)
O009	C00F	1.270(3)
O00A	C00F	1.261(3)
N00B	C00J	1.335(3)
N00B	C00J1	1.335(3)
C00E	C00L	1.509(3)
C00F	C00N	1.511(3)
N00G	C00I	1.141(5)
C00H	C00O	1.374(3)
C00H	C00O1	1.374(3)
C00I	C00M	1.458(5)
C00J	C00O	1.375(3)
C00K	C00Q	1.386(4)
C00K	N00E	1.338(3)
C00Q	C00T	1.303(13)
C00Q	C00U	1.443(11)
C00R	C00W	1.391(10)
C00R	N00E	1.350(11)
C00T	C00W	1.405(13)
N00E	C4	1.376(10)
C4	C00X	1.383(9)
C00X	C00U	1.358(11)
N2	C31	1.312(12)
N2	C3	1.312(12)
N2	C7	1.366(12)
N2	C71	1.366(12)
N2	C3a1	1.269(14)
N2	C3a	1.269(14)
N2	C7a1	1.465(14)
N2	C7a	1.465(14)
C3	C1	1.388(11)
C1	C51	1.343(11)
C5	C6	1.379(11)
C5	C61	1.379(11)
C6	C7	1.385(11)
C3a	C1a	1.472(15)
C1a	C5a	1.177(15)
C5a	C6a	1.464(13)
C6a	C7a	1.404(14)

Table S14. Bond Angles in ° for Co4O4OAc4Py4.

Atom	Atom	Atom	Angle/°
Co031	Co01	Co021	63.106(14)
O0004	Co01	Co021	44.05(4)
O0004	Co01	Co031	43.35(4)
O0051	Co01	Co021	43.72(6)
O0051	Co01	Co031	87.63(5)
O0051	Co01	O0004	87.09(7)
O0061	Co01	Co021	88.33(5)
O0061	Co01	Co031	44.12(6)
O0061	Co01	O0004	86.96(7)
O0061	Co01	O0051	81.77(7)
O0007	Co01	Co021	84.05(5)
O0007	Co01	Co031	131.46(4)
O0007	Co01	O0004	88.13(6)
O0007	Co01	O0051	92.11(7)
O0007	Co01	O0061	172.33(7)
O0091	Co01	Co021	132.54(5)
O0091	Co01	Co031	83.62(5)
O0091	Co01	O0004	88.49(6)
O0091	Co01	O0051	170.80(7)
O0091	Co01	O0061	89.94(7)
O0091	Co01	O0007	95.81(7)
N00E	Co01	Co021	136.66(6)
N00E	Co01	Co031	138.04(6)
N00E	Co01	O0004	178.31(7)
N00E	Co01	O0051	93.87(8)
N00E	Co01	O0061	94.56(9)
N00E	Co01	O0007	90.44(7)
N00E	Co01	O0091	90.76(7)
Co01	Co02	Co011	63.107(16)
Co03	Co02	Co01	58.369(13)
Co03	Co02	Co011	58.369(13)
O0041	Co02	Co011	43.23(4)
O0004	Co02	Co01	43.23(4)
O0041	Co02	Co01	87.20(4)
O0004	Co02	Co011	87.20(4)
O0041	Co02	Co03	40.52(4)
O0004	Co02	Co03	40.52(4)
O0004	Co02	O0041	81.01(9)
O0005	Co02	Co011	43.59(4)
O0005	Co02	Co01	43.59(4)
O0005	Co02	Co03	83.80(6)
O0005	Co02	O0041	86.14(6)
O0005	Co02	O0004	86.14(6)
O0008	Co02	Co01	83.34(4)
O0008	Co02	Co011	131.87(5)
O0081	Co02	Co01	131.87(5)
O0081	Co02	Co011	83.34(4)
O0008	Co02	Co03	130.95(5)
O0081	Co02	Co03	130.95(5)
O0081	Co02	O0041	90.78(6)
O0008	Co02	O0004	90.78(6)
O0081	Co02	O0004	170.36(6)
O0008	Co02	O0041	170.36(6)
O0081	Co02	O0005	88.29(6)
O0008	Co02	O0005	88.29(6)
O0008	Co02	O0081	96.92(9)
N00B	Co02	Co01	136.36(5)
N00B	Co02	Co011	136.36(5)
N00B	Co02	Co03	96.12(7)
N00B	Co02	O0004	93.80(7)
N00B	Co02	O0041	93.80(7)
N00B	Co02	O0005	179.92(10)
N00B	Co02	O0081	91.76(7)
N00B	Co02	O0008	91.76(7)
Co01	Co03	Co011	63.225(17)
Co02	Co03	Co01	58.525(13)
Co02	Co03	Co011	58.525(13)
O0041	Co03	Co011	43.29(4)
O0004	Co03	Co01	43.29(4)
O0004	Co03	Co011	87.85(4)
O0041	Co03	Co01	87.85(4)
O0041	Co03	Co02	41.20(4)
O0004	Co03	Co02	41.20(4)
O0004	Co03	O0041	82.38(9)
O0006	Co03	Co011	44.10(4)
O0006	Co03	Co01	44.10(4)
O0006	Co03	Co02	84.70(7)
O0006	Co03	O0041	86.87(6)
O0006	Co03	O0004	86.87(6)
O00A1	Co03	Co011	131.48(5)
O00A	Co03	Co01	131.48(5)
O00A	Co03	Co011	83.80(5)
O00A1	Co03	Co01	83.80(5)
O00A	Co03	Co02	132.04(5)
O00A1	Co03	Co02	132.04(5)
O00A	Co03	O0041	91.23(6)
O00A	Co03	O0004	171.64(7)
O00A1	Co03	O0004	91.23(6)
O00A1	Co03	O0041	171.64(7)
O00A1	Co03	O0006	87.40(7)
O00A	Co03	O0006	87.40(7)
O00A1	Co03	O00A	94.59(9)
N2	Co03	Co01	136.76(5)
N2	Co03	Co011	136.76(5)
N2	Co03	Co02	96.62(8)
N2	Co03	O0041	94.12(7)
N2	Co03	O0004	94.12(7)
N2	Co03	O0006	178.69(10)
N2	Co03	O00A1	91.71(7)
N2	Co03	O00A	91.71(7)
Co021	O0004	Co01	92.72(6)
Co031	O0004	Co01	93.36(6)
Co031	O0004	Co021	98.28(7)
Co01	O0005	Co011	98.61(9)
Co02	O0005	Co011	92.69(7)
Co02	O0005	Co01	92.69(7)
Co01	O0006	Co011	97.68(10)
Co03	O0006	Co01	91.78(7)
Co03	O0006	Co011	91.78(7)
C00E	O0007	Co01	122.51(14)
C00E	O0008	Co021	121.39(14)
C00F	O0009	Co011	122.34(15)
C00F	O00A	Co03	122.17(15)
C00J1	N00B	Co02	121.36(13)
C00J	N00B	Co02	121.36(13)
C00J1	N00B	C00J	117.2(3)
O0008	C00E	O0007	128.2(2)
C00L	C00E	O0007	115.4(2)
C00L	C00E	O0008	116.4(2)
O00A	C00F	O0009	127.6(2)
C00N	C00F	O0009	116.1(2)
C00N	C00F	O00A	116.3(2)
C00O1	C00H	C00O	118.3(3)
C00M	C00I	N00G	179.9(5)
C00O	C00J	N00B	123.1(2)
N00E	C00K	C00Q	122.7(3)
C00J	C00O	C00H	119.2(2)
C00T	C00Q	C00K	121.3(6)
C00U	C00Q	C00K	115.8(5)
C00U	C00Q	C00T	18.1(6)
N00E	C00R	C00W	122.6(9)
C00W	C00T	C00Q	117.7(9)

Atom	Atom	Atom	Angle/°
C00T	C00W	C00R	118.9(8)
C00K	N00E	Co01	122.48(18)
C00R	N00E	Co01	120.7(5)
C00R	N00E	C00K	115.6(5)
C4	N00E	Co01	117.0(4)
C4	N00E	C00K	119.9(4)
C4	N00E	C00R	19.9(5)
C00X	C4	N00E	120.7(7)
C00U	C00X	C4	119.0(7)
C00X	C00U	C00Q	121.3(7)
C3	N2	Co03	119.3(6)
C31	N2	Co03	119.3(6)
C31	N2	C3	115.9(14)
C71	N2	Co03	121.5(6)
C7	N2	Co03	121.5(6)
C71	N2	C31	119.1(8)
C7	N2	C31	20.4(12)
C71	N2	C3	20.4(12)
C7	N2	C3	119.1(8)
C71	N2	C7	114.2(12)
C3a	N2	Co03	130.4(7)
C3a1	N2	Co03	130.4(7)
C3a	N2	C31	104.5(7)
C3a1	N2	C31	11.6(11)
C3a1	N2	C3	104.5(7)
C3a	N2	C3	11.6(11)
C3a1	N2	C7	24.0(10)
C3a	N2	C71	24.0(10)
C3a	N2	C7	107.7(8)
C3a1	N2	C71	107.7(8)
C3a1	N2	C3a	93.0(14)

Atom	Atom	Atom	Angle/°
C7a1	N2	Co03	112.4(6)
C7a	N2	Co03	112.4(6)
C7a	N2	C31	23.8(10)
C7a1	N2	C31	128.3(8)
C7a	N2	C3	128.3(8)
C7a1	N2	C3	23.8(10)
C7a1	N2	C71	9.3(10)
C7a1	N2	C7	122.2(6)
C7a	N2	C71	122.2(6)
C7a	N2	C7	9.3(10)
C7a	N2	C3a	117.0(9)
C7a1	N2	C3a1	117.0(9)
C7a	N2	C3a1	30.7(11)
C7a1	N2	C3a	30.7(11)
C7a1	N2	C7a	129.7(13)
C1	C3	N21	121.0(11)
C51	C1	C3	120.7(11)
C1	C5	C11	113.6(15)
C6	C5	C11	21.4(8)
C61	C5	C1	21.4(8)
C6	C5	C1	119.5(13)
C61	C5	C11	119.5(13)
C61	C5	C6	116.6(17)
C7	C6	C5	118.0(13)
C6	C7	N2	121.7(12)
C1a	C3a	N21	123.5(12)
C5a	C1a	C3a	122.4(11)
C6a	C5a	C1a	119.9(10)
C7a	C6a	C5a	119.5(11)
C6a	C7a	N2	117.6(11)

Table S15. Torsion Angles in ˚ for $Co_4O_4OAc_4Py_4$.

Atom	Atom	Atom	Atom	Angle/°
Co01	O007	C00E	O008	-0.50(17)
Co01	O007	C00E	C00L	179.56(17)
Co011	O009	C00F	O00A	-7.78(17)
Co011	O009	C00F	C00N	171.68(16)
Co01	N00E	C00K	C00Q	-180.0(2)
Co01	N00E	C00R	C00W	174.4(6)
Co01	N00E	C4	C00X	-177.6(5)
Co02	O008	C00E	O007	-6.16(17)
Co021	O008	C00E	O007	-6.16(17)
Co02	O008	C00E	C00L	173.78(17)
Co021	O008	C00E	C00L	173.78(17)
Co02	N00B	C00J1	C00O1	176.0(2)
Co02	N00B	C00J	C00O	-176.0(2)
Co03	O00A	C00F	O009	2.37(17)
Co031	O00A	C00F	O009	2.37(17)
Co03	O00A	C00F	C00N	-177.08(16)
Co031	O00A	C00F	C00N	-177.08(16)
Co03	N2	C3	C1	173.4(9)
Co03	N2	C31	C11	-173.4(9)
Co03	N2	C7	C6	-174.3(9)
Co03	N2	C71	C61	174.3(9)
Co03	N2	C3a1	C1a1	-177.0(12)
Co03	N2	C3a	C1a	177.0(12)
Co03	N2	C7a	C6a	-178.1(9)
Co03	N2	C7a1	C6a1	178.1(9)
N00B	C00J	C00O	C00H	-1.1(4)
N00B1	C00J	C00O	C00H	-1.1(4)
C00K	C00Q	C00T	C00W	-7.9(7)
C00K	C00Q	C00U	C00X	-0.5(6)
C00K	N00E	C00R	C00W	6.6(6)
C00K	N00E	C4	C00X	-6.7(6)
C00Q	C00T	C00W	C00R	2.3(11)
C00Q	C00U	C00X	C4	3.1(10)
C00R	N00E	C4	C00X	76(2)
N00E	C4	C00X	C00U	0.4(9)
N2	C3	C1	C51	2(3)
N2	C31	C11	C5	-2(3)
N21	C7	C6	C5	0.3(18)
N2	C7	C6	C5	0.3(18)
N2	C3a	C1a	C5a	-2(2)
N21	C3a	C1a	C5a	-2(2)
N21	C7a	C6a	C5a	2.5(18)
N2	C7a	C6a	C5a	2.5(18)
C3	C1	C51	C11	-22.4(10)
C3	C1	C51	C6	0.7(13)
C3	C1	C51	C61	89(4)
C11	C5	C6	C7	78(3)
C1	C51	C6	C7	-2(2)
C3a	C1a	C5a	C6a	1.5(17)
C1a	C5a	C6a	C7a	-1.7(17)

Table S16. Hydrogen Fractional Atomic Coordinates (×10⁴) and Equivalent Isotropic Displacement Parameters (Å²×10³) for $Co_4O_4OAc_4Py_4$. U_{eq} is defined as 1/3 of the trace of the orthogonalised U_{ij}.

Atom	x	y	z	Ueq
H00H	2086.6(19)	1735(2)	5000	56.0(9)
H00J	2664.9(15)	4133.3(17)	3549.2(18)	61.8(7)
H00K	2180.0(16)	9246.1(16)	6443.5(19)	64.1(8)
H00a	4181(9)	6213(4)	8119(9)	86.0(10)
H00b	3876(5)	5141(11)	8074(9)	86.0(10)
H00c	4521(4)	5421(14)	7412(2)	86.0(10)
H00i	5517(12)	5941(3)	4544(19)	83.9(14)
H00l	5263(17)	5965(3)	5669(5)	83.9(14)
H00m	4722(6)	6016(3)	4790(20)	83.9(14)
H00d	1040.8(14)	8085.3(18)	1923(2)	84.4(10)
H00e	533.5(14)	7217.5(18)	2186(2)	84.4(10)
H00f	493.7(14)	8211.8(18)	2789(2)	84.4(10)
H00O	2264.2(17)	2563.8(18)	3511(2)	70.4(9)
H00Q	2651.7(19)	10738.6(19)	6809(2)	80.6(9)
H00g	2652.0(19)	10797.6(19)	6609(2)	80.6(9)
H00R	3983(5)	8202(8)	5813(8)	65(2)
H00T	3731(6)	11072(8)	6337(9)	83(2)
H00W	4448(5)	9750(6)	5908(8)	79(2)
H4	4009(5)	8036(6)	6277(7)	70(2)
H00X	4534(4)	9525(5)	6565(8)	89(2)
H00U	3876(5)	10903(7)	6674(8)	86(2)
H3	964(9)	5211(11)	6422(10)	50(2)
H1	279(6)	3839(8)	6432(8)	45(2)
H5	104(11)	2972(14)	5009.703133	43(3)
H6	636(8)	3463(11)	3539(10)	52(2)
H7	1293(9)	4872(10)	3560(10)	50(2)
H3a	816(9)	5061(12)	6314(11)	51(3)
H1a	246(7)	3557(10)	6094(10)	53(3)
H5a	201(6)	2855(8)	4710(7)	37(3)
H6a	797(7)	3523(10)	3302(10)	50(2)
H7a	1371(9)	5025(11)	3470(11)	50(2)

Table S17. Atomic Occupancies for all atoms that are not fully occupied in $Co_4O_4OAc_4Py_4$.

Atom	Occupancy
H00K	0.545(14)
H00i	0.500000
H00l	0.500000
H00m	0.500000
H00Q	0.455(14)
H00g	0.545(14)
C00R	0.455(14)
H00R	0.455(14)
C00T	0.455(14)
H00T	0.455(14)
C00W	0.455(14)
H00W	0.455(14)
C4	0.545(14)
H4	0.545(14)
C00X	0.545(14)
H00X	0.545(14)
C00U	0.545(14)
H00U	0.545(14)
C3	0.250000
H3	0.250000
C1	0.250000
H1	0.250000
C5	0.250000
H5	0.250000
C6	0.250000
H6	0.250000
C7	0.250000
H7	0.250000
C3a	0.250000
H3a	0.250000
C1a	0.250000
H1a	0.250000
C5a	0.250000
H5a	0.250000
C6a	0.250000
H6a	0.250000
C7a	0.250000
H7a	0.250000

Table S18. Solvent masking (PLATON/SQUEEZE) information for $Co_4O_4OAc_4Py_4$.

No	x	y	z	V	e	Content
1	0.000	0.000	0.500	107.9	33.0	2MeCN
2	0.500	0.500	0.000	107.9	33.0	2MeCN

8. References

1 R. K. Harris, E. D. Becker, S. M. Cabral de Menezes, R. Goodfellow and P. Granger, *Pure Appl. Chem.*, 2001, **73**, 1795–1818.
2 R. K. Harris, E. D. Becker, S. M. Cabral de Menezes, P. Granger, R. E. Hoffman and K. W. Zilm, *Pure Appl. Chem.*, 2008, **80**, 59–84.
3 R. Chakrabarty, S. J. Bora and B. K. Das, *Inorg. Chem.*, 2007, **46**, 9450–9462.
4 A. I. Nguyen, K. M. Van Allsburg, M. W. Terban, M. Bajdich, J. Oktawiec, J. Amtawong, M. S. Ziegler, J. P. Dombrowski, K. V. Lakshmi, W. S. Drisdell, J. Yano, S. J. L. Billinge and T. D. Tilley, *Proc. Natl. Acad. Sci.*, 2019, **116**, 201815013.
5 A. Yamasaki, *J. Coord. Chem.*, 1991, **24**, 211–260.
6 WSolids1 ver. 1.20.20, K.Eichele, 2013.
7 D. Massiot, F. Fayon, M. Capron, I. King, S. Le Calvé, B. Alonso, J.-O. Durand, B. Bujoli, Z. Gan and G. Hoatson, *Magn. Reson. Chem.*, 2002, **40**, 70–76.
8 S. G. J. van Meerten, W. M. J. Franssen and A. P. M. Kentgens, *J. Magn. Reson.*, 2019, **301**, 56–66.
9 V. N. Staroverov, G. E. Scuseria, J. Tao and J. P. Perdew, *J. Chem. Phys.*, 2003, **119**, 12129–12137.
10 J.-D. Chai and M. Head-Gordon, *Phys. Chem. Chem. Phys.*, 2008, **10**, 6615.
11 F. Weigend and R. Ahlrichs, *Phys. Chem. Chem. Phys.*, 2005, **7**, 3297.
12 J. K. Beattie, T. W. Hambley, J. A. Klepetko, A. F. Masters and P. Turner, *Polyhedron*, 1998, **17**, 1343–1354.
13 I. G. Shenderovich, *J. Chem. Phys.*, 2018, **148**, 124313.
14 M. J. Duer, Ed., *Solid-State NMR Spectroscopy Principles and Applications*, Wiley, 2001.
15 D. L. Bryce, G. M. Bernard, M. Gee, M. D. Lumsden, K. Eichele and R. E. Wasylishen, *Can. J. Anal. Sci. Spectrosc.*, 2001, **46**, 46–82.
16 I. G. Shenderovich and H.-H. Limbach, *Solids*, 2021, **2**, 139–154.
17 I. G. Shenderovich, *J. Phys. Chem. A*, 2023, **127**, 5547–5555.
18 I. G. Shenderovich, *ChemPhysChem*, , DOI:10.1002/cphc.202300986.
19 I. Hung, P. Gor'kov and Z. Gan, *J. Chem. Phys.*, , DOI:10.1063/1.5126599.
20 A. P. M. Kentgens, *Geoderma*, 1997, **80**, 271–306.
21 P. Granger, in *Encyclopedia of Magnetic Resonance*, John Wiley & Sons, Ltd, Chichester, UK, 2007.
22 B. P. Tatman, H. Modha and S. P. Brown, *J. Magn. Reson.*, 2023, **352**, 107459.
23 M. Schwarze, M. Schröder, D. Stellmach, K. Kailasam, A. Thomas and R. Schomäcker, *Chemie Ing. Tech.*, 2013, **85**, 500–507.
24 M. Schwarze, D. Stellmach, M. Schröder, K. Kailasam, R. Reske, A. Thomas and R. Schomäcker, *Phys. Chem. Chem. Phys.*, 2013, **15**, 3466.
25 N. S. McCool, D. M. Robinson, J. E. Sheats and G. C. Dismukes, *J. Am. Chem. Soc.*, 2011, **133**, 11446–11449.
26 A. Genoni, G. La Ganga, A. Volpe, F. Puntoriero, M. Di Valentin, M. Bonchio, M. Natali and A. Sartorel, *Faraday Discuss.*, 2015, **185**, 121–141.
27 S. Berardi, G. La Ganga, M. Natali, I. Bazzan, F. Puntoriero, A. Sartorel, F. Scandola, S. Campagna and M. Bonchio, *J. Am. Chem. Soc.*, 2012, **134**, 11104–11107.
28 P. F. Smith, C. Kaplan, J. E. Sheats, D. M. Robinson, N. S. McCool, N. Mezle and G. C. Dismukes, *Inorg. Chem.*, 2014, **53**, 2113–2121.
29 S. R. Chaudhari, D. Wisser, A. C. Pinon, P. Berruyer, D. Gajan, P. Tordo, O. Ouari, C. Reiter, F. Engelke, C. Copéret, M. Lelli, A. Lesage and L. Emsley, *J. Am. Chem. Soc.*, 2017, **139**, 10609–10612.
30 F. M. Wisser, M. Duguet, Q. Perrinet, A. C. Ghosh, M. Alves-Favaro, Y. Mohr, C. Lorentz, E. A. Quadrelli, R. Palkovits, D. Farrusseng, C. Mellot-Draznieks, V. Waele and J. Canivet, *Angew. Chemie Int. Ed.*, 2020, **59**, 5116–5122.
31 A. I. Nguyen, J. Wang, D. S. Levine, M. S. Ziegler and T. D. Tilley, *Chem. Sci.*, 2017, **8**, 4274–4284.
32 G. M. Sheldrick, *Acta Crystallogr. Sect. A Found. Adv.*, 2015, **71**, 3–8.
33 O. V. Dolomanov, L. J. Bourhis, R. J. Gildea, J. A. K. Howard and H. Puschmann, *J. Appl. Crystallogr.*, 2009, **42**, 339–341.
34 L. J. Bourhis, O. V. Dolomanov, R. J. Gildea, J. A. K. Howard and H. Puschmann, *Acta Crystallogr. Sect. A Found. Adv.*, 2015, **71**, 59–75.
35 CrysAlisPro (V43), Rigaku Oxford Diffraction Ltd., 2019.
36 F. Kleemiss, O. V. Dolomanov, M. Bodensteiner, N. Peyerimhoff, L. Midgley, L. J. Bourhis, A. Genoni, L. A. Malaspina, D. Jayatilaka, J. L. Spencer, F. White, B. Grundkötter-Stock, S. Steinhauer, D. Lentz, H. Puschmann and S. Grabowsky, *Chem. Sci.*, 2021, **12**, 1675–1692.